

Search for physics beyond the Standard Model in diphoton final states at CMS

Chiara Rovelli^{*†}

INFN Roma

E-mail: chiara.rovelli@cern.ch

A search for the resonant production of high mass photon pairs is presented. The search focuses on spin-0 and spin-2 resonances with an invariant mass between 0.5 TeV and 4.5 TeV and with a width, relative to the mass, between 1.4×10^{-4} and 5.6×10^{-2} . The results are based on proton-proton collision data at a center-of-mass energy of 13 TeV collected by the CMS experiment at the LHC and corresponding to an integrated luminosity of 12.9 fb^{-1} . The results of the search are combined statistically with those previously obtained by CMS at $\sqrt{s} = 8 \text{ TeV}$ and $\sqrt{s} = 13 \text{ TeV}$, in 2012 and 2015. No significant excess with respect to the Standard Model expectation is observed. Limits are set on scalar resonances produced through gluon-gluon fusion and on Randall–Sundrum gravitons.

38th International Conference on High Energy Physics

3-10 August 2016

Chicago, USA

^{*}Speaker.

[†]on behalf of the CMS Collaboration

1. Introduction

The resonant production of high mass photon pairs is predicted in several extensions of the Standard Model (SM) of particle physics. The spin of a resonance which decays to two photons must be either 0 or an integer greater than or equal to 2. Spin-2 resonances decaying to a photon pair are predicted in models like the one proposed by Randall and Sundrum [1] (RS), which advocates additional space-like dimensions as a solution to the hierarchy problem. Spin-0 resonances are predicted in simple extensions of the SM Higgs sector, like the two-Higgs-doublet model [2]. Recently, the ATLAS [3] and CMS [4] Collaborations published results based on collision data at a center-of-mass energy $\sqrt{s} = 13$ TeV collected in 2015 and corresponding to an integrated luminosity of about 3 fb^{-1} per experiment. Both analyses reported the observation of a modest deviation from the background-only expectation, compatible with the production of a resonance with a mass around 750 GeV. In this Proceeding we discuss an update based on data collected in 2016 by CMS at $\sqrt{s} = 13$ TeV and corresponding to an integrated luminosity of 12.9 fb^{-1} [5]. The results of the search are also combined statistically with those previously obtained by CMS at $\sqrt{s} = 8$ TeV and 13 TeV, in 2012 [6] and 2015 [4].

2. The CMS detector

A detailed description of the CMS detector, together with a definition of the coordinate system used and the standard kinematic variables, can be found in [7].

The central feature of the CMS apparatus is a superconducting solenoid of 6 m internal diameter, providing a magnetic field of 3.8 T. Within the superconducting solenoid volume are a silicon pixel and strip tracker, an electromagnetic calorimeter (ECAL), and a brass/scintillator hadron calorimeter, each one composed of a barrel and two endcap sections. Muons are measured in gas-ionization detectors embedded in the steel flux-return yoke outside the solenoid. Extensive forward calorimetry complements the coverage provided by the barrel and endcap detectors.

The main detector component used in this analysis is the ECAL, which is a homogeneous calorimeter made of lead tungstate scintillating crystals. In the barrel (endcaps) section of the ECAL, an energy resolution of about 1% (2.5%) is achieved for unconverted or late-converting photons [8]. Given the large amount of material between the interaction point and the ECAL (from 0.4 to almost 2 radiation lengths X_0) the probability of photon conversions before reaching the ECAL is large.

3. Event selection and reconstruction

Despite a large non-resonant background, the diphoton decay mode provides a clean final-state topology and the mass of the decaying object can be reconstructed with high precision. This analysis consists in a search for a localised excess of events in the diphoton mass spectrum.

Events are selected online requiring at least two photon candidates with transverse momentum $p_T > 60$ GeV, and ratio between the energy deposited in the HCAL towers behind the photon and the photon energy (H/E) compatible with the one expected for electromagnetic candidates.

Offline, photons are reconstructed from the energy deposits in the ECAL. A dedicated clustering algorithm is used, which clusters together the energy deposits compatible with the expected shower

shape of a photon. The energy of the photon candidates is assigned using a multivariate regression, which is tuned on Monte Carlo. Discrepancies in the photon energy scale and resolution between data and simulation are resolved using $Z \rightarrow e^+e^-$ events. The needed corrections to the energy scale are applied to photons in data. Since the energy resolution in data is worse than predicted from simulation, an additional Gaussian smearing is applied to simulated photons.

To be considered for the analysis, the photon candidates are required to have $p_T > 75$ GeV and to be in the ECAL fiducial region (i.e. $|\eta| < 2.5$, with the exclusion of the transition region between the barrel and the endcaps, $1.44 < |\eta| < 1.57$). They have to be isolated from charged particles and from additional photon candidates with the following definitions: the sum of the p_T of the charged hadron candidates within a cone with $\Delta R = \sqrt{(\Delta\eta)^2 + (\Delta\phi)^2} = 0.3$ around the photon must be smaller than 5 GeV, excluding from the sum all charged hadron candidates not assigned to the selected interaction vertex or compatible with conversion tracks associated with the photon; the sum of the transverse energy of additional photon candidates within $\Delta R = 0.3$ is required to be below 2.5 GeV, after a correction for the effect of additional interactions in the bunch crossing is applied. Furthermore, the photon candidates have to pass some identification criteria based on the transverse size of the electromagnetic cluster in the η direction and on H/E (< 0.05). Finally the candidates are rejected if they are associated with an electron track incompatible with a photon conversion. The efficiency of these identification criteria is above 90 (85)% in the barrel (endcaps) for isolated photons in the p_T range which is considered for the analysis. In data the online and offline selection efficiencies are measured using events with a Z boson decaying to a pair of electrons, or to a pair of electrons or muons in association with a photon. The offline efficiencies measured in data are 3.5% and 6.5% lower than those estimated from simulation for photons in the barrel and in the endcaps respectively. A correction factor is applied to simulated events to take this difference into account. Once photons are selected, pairs are built where at least one of the photon candidates has $|\eta| < 1.44$. In case more than one photon pair satisfies the selection the one with the largest scalar sum of photon momenta is kept. The selected photon pairs are split into two categories: the first (EBEB) containing pairs where both candidates are in the ECAL barrel, and the second (EBEE) with pairs where one of the candidates is reconstructed in the endcaps. Finally, diphoton events in the EBEB (EBEE) category are retained when the invariant mass $m_{\gamma\gamma}$ of the selected photon pair satisfies $m_{\gamma\gamma} > 230$ GeV (330 GeV). The signal region is defined for both categories as $m_{\gamma\gamma} > 500$ GeV. The fraction of selected signal events varies between 0.5 and 0.7 depending on the signal hypothesis. The diphoton mass resolution depends on the precision of the measurement of the photon energies and of the angle between the two photons. If the interaction vertex is known within 10 mm the latter gives a negligible contribution to the mass resolution, therefore an accurate reconstruction of the interaction vertex is important in this search. The same algorithm proposed in [9] is used, which combines informations on the transverse momentum of the recoiling tracks, on the correlation between the two photons and the recoiling tracks and on the reconstructed conversions if available. The fraction of events in which the interaction vertex is reconstructed within 10 mm is about 90% for resonances with mass above 500 GeV.

4. Interpretation and results

The diphoton invariant mass distribution of the selected events is shown in Fig. 1 for the two

analysis categories.

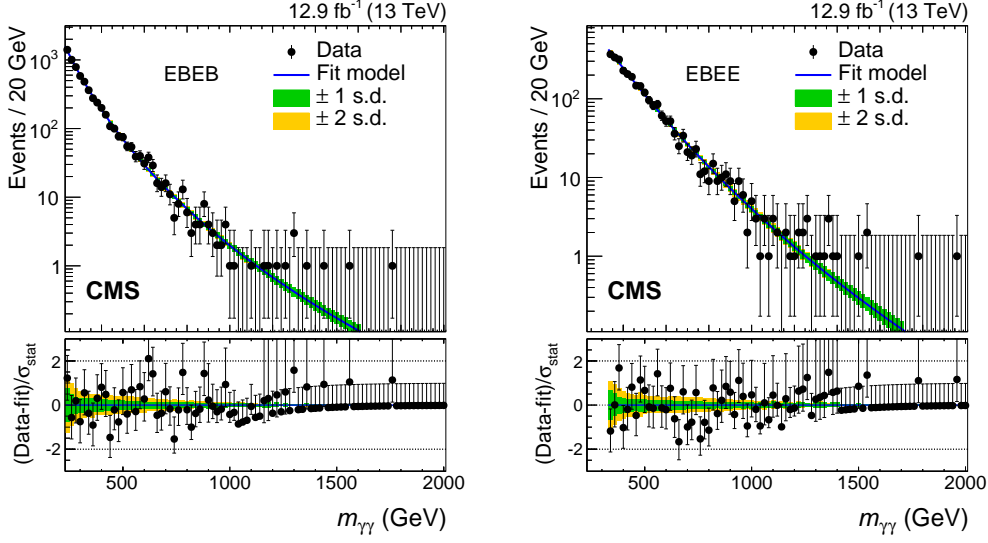


Figure 1: Observed invariant mass spectra for events selected in the EBEB (left) and EBEE (right) categories. The solid lines and the shaded bands show the results of likelihood fits to the data together with the associated 1 and 2 standard deviation uncertainty bands. The ratio of the difference between the data and the fit to the statistical uncertainty in the data is given in the lower plots.

The results of the search are interpreted in the framework of a composite statistical hypothesis test. A simultaneous fit to the invariant mass spectra of the EBEB and EBEE event categories is used to study the compatibility of the data with the background-only and the signal+background hypotheses. The signal distribution in $m_{\gamma\gamma}$ used in the fit is determined from the convolution of the intrinsic shape of the resonance, derived using the PYTHIA generator, and the ECAL detector response. The signal mass resolution is about 1% (1.5%) for EBEB (EBEE) events. The background $m_{\gamma\gamma}$ spectrum is described by a parametric function with coefficients obtained from a fit to the data events. The accuracy of the function is assessed using Monte Carlo simulations and it is quantified by studying the difference between the true and predicted number of background events in several $m_{\gamma\gamma}$ intervals in the search region. Based on the result of this test, an uncertainty is added in the likelihood function which has the effect of avoiding falsely positive or negative tests that could be induced by a mismodeling of the background shape. The main uncertainty affecting the analysis is the statistical one. For what concern the systematics, a 6.2% uncertainty is assigned related to the knowledge of the integrated luminosity, a 6% one related to the selection efficiency and a 6% one for the choice of the PDFs. The assumed uncertainties on the photon energy scale and resolution are 1% and 10% respectively.

The modified frequentist method CLs is used to set upper limits on the resonant diphoton production rate. The compatibility of the observation with the background-only hypothesis is evaluated computing the background-only p-value. In both cases asymptotic formulas are used.

Expected and observed upper limits on the production of scalar and RS graviton resonances are computed. Using the LO cross sections from PYTHIA 8.2, RS gravitons with masses m_X below 1.75, 3.75, and 4.35 TeV are excluded for width relative to the mass ratios $\Gamma_X/m_X = 1.4 \times 10^{-4}$,

1.4×10^{-2} , and 5.6×10^{-2} . The largest excess is observed for m_X of about 620 GeV, with a local significance of roughly 2.4 and 2.7 standard deviations for narrow spin-0 and RS graviton signal hypotheses respectively. After taking into account the effect of searching for several signal hypotheses, the significance of the excess is reduced to less than one standard deviation. No excess is observed close to $m_X=750$ GeV, where a modest deviation from the background-only expectation was observed in the dataset collected in 2015.

5. Combination with previous results

The results discussed so far are combined statistically with those reported in [4], where a total of 19.7 fb^{-1} recorded at $\sqrt{s} = 8 \text{ TeV}$ in 2012 and 3.3 fb^{-1} recorded at $\sqrt{s} = 13 \text{ TeV}$ in 2015 are analyzed. The combination procedure and the correlation model between uncertainties is detailed in [5]. The ratio of the 8 TeV to the 13 TeV production rate is computed using PYTHIA 8.2. The cross-section ratio decreases from 0.27 and 0.29 at $m_X = 500 \text{ GeV}$ to 0.03 and 0.04 at $m_X = 4 \text{ TeV}$, for the scalar and RS graviton resonance respectively.

The combination is first run between the two datasets collected at $\sqrt{s} = 13 \text{ TeV}$. Compared to the 2016 dataset alone, the combined analysis sensitivity improves by roughly 10% and 20% at the high and low end of the m_X search region. The largest excess is observed for $m_X = 1.3 \text{ TeV}$ with a local significance of about 2.2 standard deviations, reduced to less than 1 standard deviation after accounting for the effect of searching for several signal hypotheses. For $m_X=750 \text{ GeV}$, the roughly 2.9σ excess observed in the 2015 dataset is reduced to about 0.8σ in the combined analysis.

The expected and observed 95% CL limits on the 13 TeV signal production cross-sections obtained combining the results at 8 TeV and 13 TeV are shown in Fig. 2. Compared to the sensitivity of the 13 TeV data, the analysis sensitivity improves by about 10% at the low end of the m_X range, while the improvement is negligible at the higher end of the range. RS gravitons with masses $m_X < 1.95 \text{ TeV}$ (excluded the region between 1.75 TeV and 1.85 TeV), $m_X < 3.85 \text{ TeV}$, and $m_X < 4.45 \text{ TeV}$ are excluded for $\Gamma_X/m_X = 1.4 \times 10^{-4}$, 1.4×10^{-2} , and 5.6×10^{-2} . These limits coincide with those obtained with 13 TeV data alone. The largest excess is observed for m_X about 0.9 TeV, with a local significance of about 2.2σ , corresponding to less than 1σ overall. For $m_X=750 \text{ GeV}$, the 3.4σ excess reported in [4] is reduced to about 1.9σ .

6. Conclusions

A search for the resonant production of high mass photon pairs has been presented. The analysis is based on a sample of proton-proton collisions collected by the CMS experiment in 2016 at $\sqrt{s} = 13 \text{ TeV}$, corresponding to an integrated luminosity of 12.9 fb^{-1} . The diphoton mass spectrum in the range $0.5 \text{ TeV} < m_X < 4.5 \text{ TeV}$ is examined to search for high mass spin-0 and spin-2 resonances. The results obtained with the 2016 dataset are combined statistically with those obtained in 2012 (at $\sqrt{s} = 8 \text{ TeV}$) and 2015 (at $\sqrt{s} = 13 \text{ TeV}$), corresponding to integrated luminosities of 19.7 fb^{-1} and 3.3 fb^{-1} respectively. Since no significant excess is observed above the predictions of the Standard Model, stringent limits on Randall–Sundrum graviton production are set.

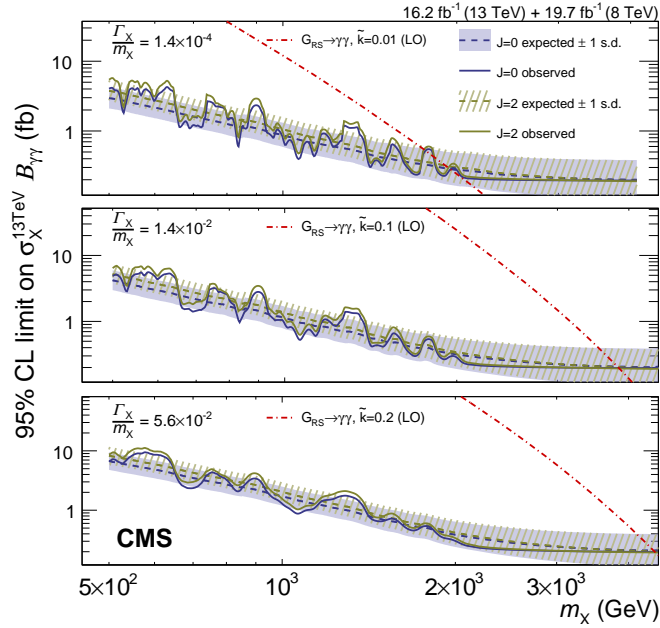


Figure 2: The 95% CL upper limits on the production of diphoton resonances as a function of the resonance mass m_X , from the combined analysis of the 8 and 13 TeV data. The 8 TeV results are scaled by the ratio of the 8 to 13 TeV cross sections. Exclusion limits for the scalar and RS graviton signals are given by the grey (darker) and green (lighter) curves, respectively. The observed limits are shown by the solid lines, while the median expected limits are given by the dashed lines together with their associated 1 standard deviation uncertainty bands. The results for (upper) a narrow width, (middle) an intermediate-width, and (lower) a broad resonance are shown.

References

- [1] L.Randall and R.Sundrum, Phys. Rev. Lett. **83**, 3370 (1999)
- [2] P.S.Bhupal Dev, A.Pilaftsis, arXiv:1408.3405
- [3] ATLAS Collaboration, JHEP 09 (2016) 001
- [4] CMS Collaboration, Phys. Rev. Lett. **117**, 051802 (2016)
- [5] CMS Collaboration, CMS-PAS-EXO-16-027, <https://cds.cern.ch/record/2205245>
- [6] CMS Collaboration, Phys. Lett. B **750**, 494 (2015)
- [7] CMS Collaboration, JINST **3** S08004 (2008)
- [8] CMS Collaboration, JINST **10** P08010 (2015)
- [9] CMS Collaboration, Eur. Phys. J. C **74** 3076 (2014)